Am J Cancer Res 2024;14(4):1815-1830
www.ajcr.us /ISSN:2156-6976/ajcr0154528

Original Article

SSH3 promotes pancreatic cancer proliferation and migration by activating the notch signaling pathway

Chengxiao Yang*, Gang Quan*, Shihang Zhang*, Jianxin Jiang

*Department of Hepatobiliary, Pancreatic and Splenic Surgery, The Tenth Affiliated Hospital, Southern Medical University (Dongguan People's Hospital), Dongguan, Guangdong, China. *Equal contributors.*

Received November 20, 2023; Accepted April 14, 2024; Epub April 15, 2024; Published April 30, 2024

Abstract: Recent studies have indicated that the dual-specificity phosphatases (DUSP) family may play a role in the advancement of pancreatic cancer. Exploring the role of the DUSP family in pancreatic cancer development and discovering novel therapeutic targets are crucial for pancreatic cancer therapy. A critical subset of 20 genes exhibiting differential expression was identified, with particular emphasis on four key genes: DUSP10, PTP4A2, SSH3, and CDKN3 by multivariate Cox proportional hazards analysis. These genes were integral to developing a novel risk model for PC, which has been independently validated as a prognostic factor for patients. To provide help for clinical treatment, we performed tumor immune analysis and predicted potential chemical drugs. Notably, our research unveiled elevated expression levels of SSH3 in human PC cells and tissues. Intriguingly, SSH3 expression correlates with the patient grade, staging, and T stage in PC. Additional studies reveal SSH3's role in enhancing PC cell proliferation and migration, intricately linked to the activation of the Notch signaling pathway. These insights provide a deeper understanding of PC pathophysiology and pave the way for novel therapeutic interventions.

Keywords: Slingshot protein phosphatase 3, pancreatic cancer, prognostic prediction, TCGA, DUSP family

Introduction

Pancreatic cancer (PC), particularly notorious for its lethality, currently exhibits a five-year survival rate of only 10%. Over the preceding 25 years, the global incidence of PC has alarmingly nearly doubled, reflecting a significant increase in its prevalence [1, 2]. There is a consensus in the literature indicating that the early detection of pancreatic ductal adenocarcinoma (PDAC) significantly correlates with improved survival outcomes in patients [3-5]. Stage I PDAC patients have a substantially longer survival rate compared to those diagnosed at later stages [6]. Cases of PDAC detected incidentally often result in greater median survival than those identified through symptomatic presentation. The primary diagnostic challenge lies in the typically asymptomatic nature of early-stage PC, resulting in a majority of cases (approximately 85%-90%) being diagnosed at advanced stages, either locally advanced (30%-35%) or metastatic (50%-55%) [7]. The high mortality in pancreatic cancer (PC) largely results from late-stage diagnosis, rendering surgical intervention infeasible. Predominant chemotherapy treatment, while initially effective in reducing tumor size, faces significant limitations due to the rapid emergence of drug resistance, underscoring the need for more effective treatment strategies [8].

The Mitogen-Activated Protein Kinase (MAPK) pathway is a critical component of cellular signaling. Its inactivation is mediated by three distinct classes of phosphatases: serine/threonine phosphatases, tyrosine phosphatases, and notably, the dual-specificity phosphatases (DUSPs) [9]. Several DUSPs possess a MAP kinase-binding motif, enabling their interaction with the MAPKs' common docking domain, a crucial aspect in regulating MAPK activity [9]. Therefore, DUSPs are subjected to complex regulation because of their importance in the regulation of MAPK activity [10]. Disruptions in DUSP regulation are frequently linked to various human diseases, particularly cancer, underscoring their potential as therapeutic targets

https://doi.org/10.62347/DAZV7194

[11]. However, the expression patterns and therapeutic relevance of DUSP family members in pancreatic cancer are not yet fully understood.

In this study, we used public databases, including The Cancer Genome Atlas (TCGA) to identify prognosis-related DUSP genes and evaluate the prognostic accuracy of the signature in patients with PC. In addition, we found that SSH3 plays a critical role in the cell proliferation, invasion and migration of PC.

Materials and methods

Data collection

The information on RNA expression was obtained from the Cancer Genome Atlas (TCGA; https://portal.gdc.cancer.gov/), which also offers details on the clinicopathological features of PC. Samples with insufficient clinicopathological or survival data were discarded before further examination. DUSP family genes were from the HUGO Gene Nomenclature Committee (HGNC; https://www.genenames.org/).

Analysis of differentially expressed genes (DEGs) in PC tissues

The Gene Expression Profiling Interactive Analysis (GEPIA; http://gepia.cancer-pku.cn/) platform was employed to discern differentially expressed DUSP family genes between PC tumors and adjacent normal tissues, adopting a threshold of |LogFC| > 1 with an adjusted *P*-value < 0.05 for identifying DEGs.

Identification of gene prognostic signatures for PC

We employed R software, utilizing univariate Cox regression analysis to explore the association between gene expression levels and overall survival in pancreatic cancer, setting a significance threshold of $P < 0.05$ for potential predictive gene identification. Advanced analyses were conducted using the 'survival' package in R, where multivariate Cox regression analysis facilitated the development of a sophisticated prognostic risk model [12]. This model yielded individualized patient risk scores, calculated through a formula that integrated the coefficients of the model. These scores enabled the categorization of patients into distinct high- and low-risk groups, based on the median risk score. We further assessed the predictive power of this risk model via Kaplan-Meier survival curves for each risk category. The model's robustness and reliability were additionally evaluated using receiver operating characteristic (ROC) curve analysis.

Development of the risk model of other clinical parameters and the prognostic nomogram

We applied both univariate and multivariate Cox regression analyses to evaluate the risk model's independence by comparing it against clinical characteristics such as grade and stage, considering $P < 0.05$ as statistically significant. Clinicopathological factors were subsequently incorporated into a prognostic nomogram.

Tumor immune analysis

The CIBERSORT algorithm was utilized to elucidate the relationship between our risk model and the levels of immune cell infiltration in pancreatic cancer [13]. We employed a suite of R packages, including 'limma', 'pheatmap', 'ggpubr', and 'vioplot', for a detailed analysis of immune cell infiltration discrepancies across varying risk groups. This study also encompassed an evaluation of immunological checkpoint expression patterns between these groups, with the results presented via comprehensive boxplots. Furthermore, to gain deeper insights into immune cell infiltration and immune-related functions in pancreatic cancer, single-sample Gene Set Enrichment Analysis (ssGSEA) was conducted, harnessing the capabilities of the 'limma', 'GSVA', and 'GSEABase' R packages.

Prediction of possible drugs for PC therapy

To identify potential compounds for pancreatic cancer (PC) therapy, we estimated the half-maximal inhibitory concentration (IC50) values of drugs listed in the Genomics of Drug Sensitivity in Cancer (GDSC) database [14]. Using the "limma", "oncoPredict", "parallel", "ggpubr", and "ggplot2" packages, the potential therapeutic compounds were identified.

Cell culture and transfection

Human pancreatic cancer cell lines (Aspc-1, Bxpc-3, MIA PaCa-2, PANC-1, and SW1990) and human normal pancreatic ductal epithelial

(HPDE) cells were cultured in Dulbecco's modified Eagle's medium (DMEM) and RPMI-1640, all with 10% fetal bovine serum. At 37 degrees Celsius, 5% CO_2 was used to cultivate all of the cells.

Cell plates were appropriately seeded, followed by the addition of small interfering RNAs (siRNAs) and Lipofectamine RNAimax (Invitrogen, 13778150) after a 12-hour incubation. The siRNAs were utilized as per the manufacturer's instructions for a duration of 24 hours. Both shRNAs and negative control (NC) RNAs were acquired from GeneChem (Shanghai, China). For shRNA transfection, Lipofectamine 2000 from Thermo Fisher Scientific was employed. Subsequently, stable cell lines expressing shSSH3 were established over a two-week period using 1 mg/mL puromycin. The sequences of the siRNAs and shRNAs used are detailed in Table S1A, S1B.

Quantitative reverse-transcriptase PCR

Utilizing the TRIzol Reagent (Invitrogen, Carlsbad, CA, USA), cell line total RNA was extracted. mRNA was discovered using the AceQ Universal SYBR qPCR Master Mix (Vazyme, Nanjing, China). We used GAPDH expression as a control. Table S1C offers a list of the primer sequences.

Western blotting

Using RIPA buffer, proteins were obtained from the pancreatic cancer cell lines and HPDE. The protein was then placed onto a 10% SDS-polyacrylamide gel electrophoresis separation gel and run on it until they were successfully separated. ECL reagents were used to find protein expression. In Table S1D, the antibodies utilized are listed.

Cell counting kit-8 analysis

After reaching 90% confluency, SSH3 siRNA-transfected PANC-1 and SW1990 cells were digesting and injected at a number of 3000 cells per well and three wells per group into 96-well culture plates. The cells were then grown and examined at 0, 24, 48, 72, and 96 h using the CCK-8 kit (WLA074, China).

EdU incorporation

The EdU combination assay was conducted using a Cell-Light EdU Apollo555 in vitro kit (Beyotime) in keeping with the manufacturer's guidelines. The cells were grown in an EdU medium for two hours after siRNA transfection.

Wound healing test

PANC-1 and SW1990 cells were seeded into 6-well plates and transfected with SSH3 siRNA. Post-transfection, the cells underwent a wound-healing assay. This involved creating a linear scratch using a 200 μL pipette tip. To get rid of cell debris, wash the cell surface with media devoid of serum. Each group's cells were then left in place for 0 and 48 h before being recorded and photographed. Finally, the range of motion of each group was then determined.

Transwell migration

50,000 cells suspended in 200 μl of cell suspension were placed in a 24-well Transwell chamber. In the bottom chamber, cultural mediums (700 μl) containing 10% FBS was added. 4 percent paraformaldehyde was kept at room temperature for 0.5 hours after 24 h, dyed with 0.5 percent crystal violet dye for 0.5 h, and the cell count was taken.

Animals

We bought male BALB/c-nude mice from the Guangdong Medical Laboratory Animal Center when they were 4 weeks old. To create the xenograft PC-bearing model, stable transfected PANC-1 cells were implanted subcutaneously into mice (5×10^6 cells/100 μl). Following the initial injection, tumor volumes were estimated as follows: volume = 1/2 length width^2. Tumor sizes and volumes were measured every four days.

Statistical analysis

All statistical analysis were performed in R (version R.4.2.1) or GraphPad Prism (version 8), and quantitative statistics are expressed as mean ± standard deviation. The student's t-test (two-tailed) was used to analyze the differences among both samples. And $P < 0.05$ was regarded significant.

Availability of data and materials

All data and materials are available. Please contact us to access if it is needed.

Results

Identification of DEGs in DUSPs from PC

Utilizing the GEPIA database, a comparative analysis of DUSP gene expression was conducted between normal (n = 171) and tumor (n = 179) pancreatic tissues. This analysis uncovered that 20 DUSP genes were notably upregulated in tumor tissues without any evidence of downregulation. These differentially expressed DUSPs include CDKN3, DUSP1, DUSP2, DUSP3, DUSP5, DUSP6, DUSP7, DUSP10, DUSP11, DUSP14, DUSP18, DUSP23, PTEN, PTP4A1, PTP4A2, PTPMT1, RNGTT, SSH1, SSH3, and STYXL1, as illustrated in **Figure 1**. Additionally, we employed the STRING database (https://cn.string-db.org/) to elucidate the interrelationships among these genes, the results of which are depicted in Figure S1.

Identification of DEGs with significant prognostic value in PC

In our study, we applied univariate Cox regression analysis to determine the prognostic impact of specific genes on overall survival in pancreatic cancer (PC). Through Cox proportional hazards analysis, 10 genes were identified as significantly associated with the survival of PC patients in the TCGA dataset (**Figure 2A**). The risk score for each patient was computed using multivariate Cox proportional hazards analysis. This calculation was based on a linear combination of the expression levels of four key genes - PTP4A2, DUSP10, CDKN3, and SSH3 - alongside their corresponding regression coefficients, following the formula: risk score = (PTP4A2 × 0.422011) + (DUSP10 × 0.267162) + (CDKN3 × 0.445569) + (SSH3 × 0.406517). This led to the stratification of 177 patients into high and low-risk groups based on the median risk score (**Figure 2B**). Higher risk scores were associated with a greater mortality risk and reduced survival times (**Figure 2C**). The expression patterns of these four genes across the risk groups are presented in **Figure 2D**. Kaplan-Meier survival analysis further highlighted that patients in the low-risk group outlived those in the high-risk group (P = 4.464e-05) (**Figure 2E**).

Evaluation of the risk model as an independent prognostic factor for PC patients

Our analyses employing univariate and multivariate Cox regression revealed that a risk model based on four genes is a significant prognostic factor for pancreatic cancer (PC) outcomes. This model demonstrated hazard ratios (HR) of 1.778 (95% CI: 1.409-2.244) in univariate and 1.792 (95% CI: 1.370-2.343) in multivariate analysis, affirming its prognostic relevance (**Figure 3A**, **3B**). Receiver Operating Characteristic (ROC) analysis further validated the model's predictive power in forecasting PC prognosis, evidenced by Area Under Curve (AUC) values of 0.681, 0.665, and 0.695 at 1, 2, and 3 years, respectively (**Figure 3C**). In addition, we developed a prognostic nomogram that integrates the risk score with key clinicopathological parameters - stage, gender, and grade - for the TCGA cohort (**Figure 3D**, **3E**). The calibration curves of the nomogram for 1-, 2-, and 3-year overall survival closely aligned with the ideal model, demonstrating its accuracy in prognostic predictions for PC patients. These collective findings underscore the robustness of our risk model as a reliable prognostic tool for PC.

Tumor microenvironment analysis

Utilizing "ggpubr", "pheatmap", "limma", and "vioplot" R packages, our immune cell infiltration analysis disclosed a notable correlation between the risk score and various immune cells, including memory B cells, CD8 T cells, activated NK cells, monocytes, and activated dendritic cells (**Figure 4A**). This association was further visualized through a bar plot, showcasing the distribution of these immune cells in both high and low-risk groups (**Figure 4B**). Additionally, we observed distinct variations in immune checkpoint expression between these groups (**Figure 4C**). Notably, the risk score exhibited significant differences across a spectrum of immune features such as CCR, MHC class I, checkpoints, inflammation promoters, B cells, CD8+ T cells, pDCs, DCs, iDCs, macrophages, mast cells, neutrophils, tumor-infiltrating lymphocytes (TILs), and regulatory T cells (Tregs), illustrated through detailed boxplots (**Figure 4D**, **4E**). This extensive analysis highlights a crucial link between the risk score and the intricate dynamics of immune cells in pancreatic cancer.

Prediction of potential chemical drugs

Predictive analyses of potential therapeutics showed distinct sensitivities to specific drugs between the risk groups. The nine most sensi-

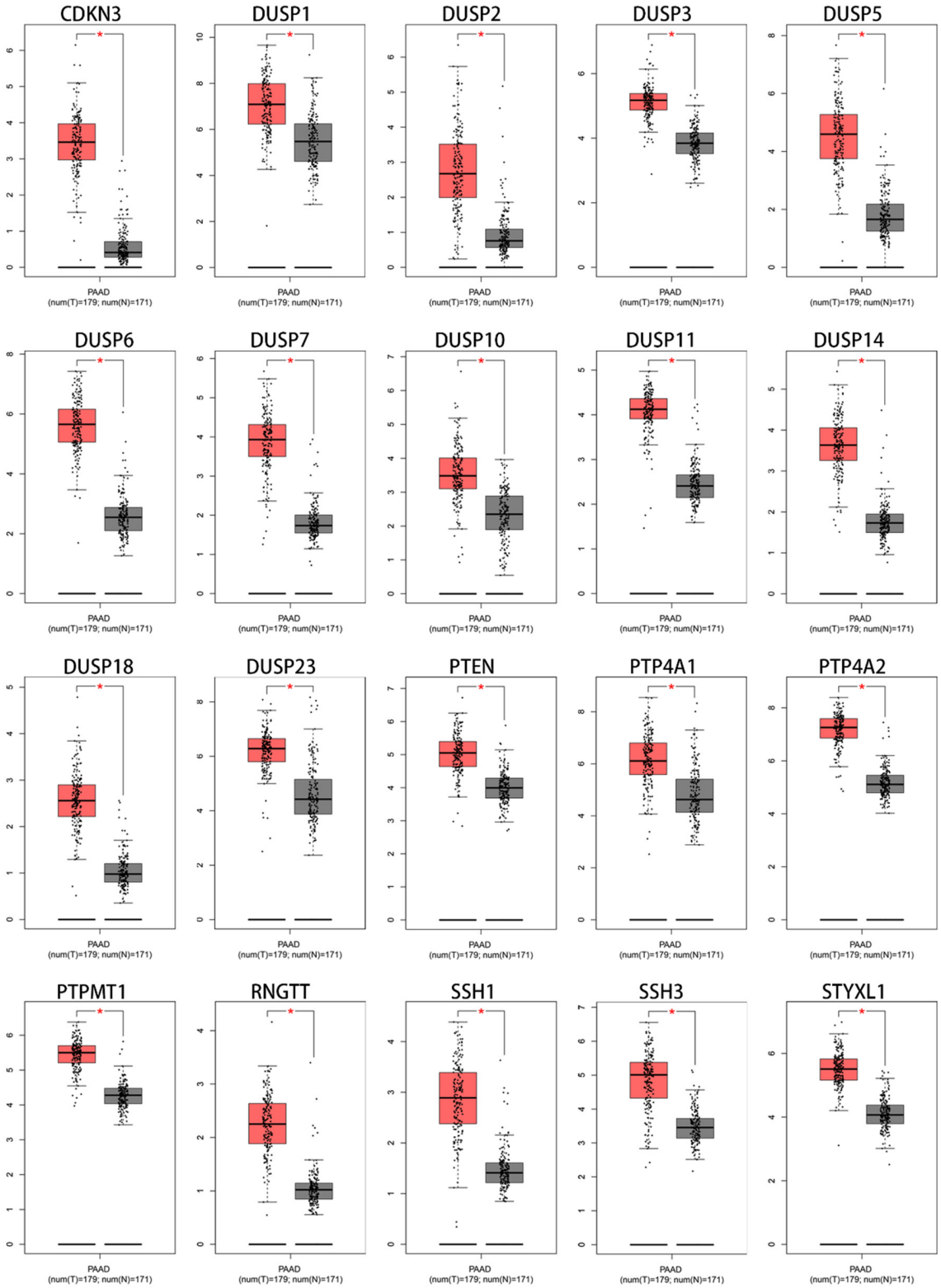

Figure 1. Expression of 20 DEGs in DUSPs in PC patients from GEPIA database (Red: Tumor; Grey: Normal). Compared with 171 normal tissues, CDKN3, DUSP1, DUSP2, DUSP3, DUSP5, DUSP6, DUSP7, DUSP10, DUSP11, DUSP14, DUSP18, DUSP23, PTEN, PTP4A1, PTP4A2, PTPMT1, RNGTT, SSH1, SSH3, and STYXL1 is highly expressed in 179 pancreatic cancer tissues. *P < 0.05.

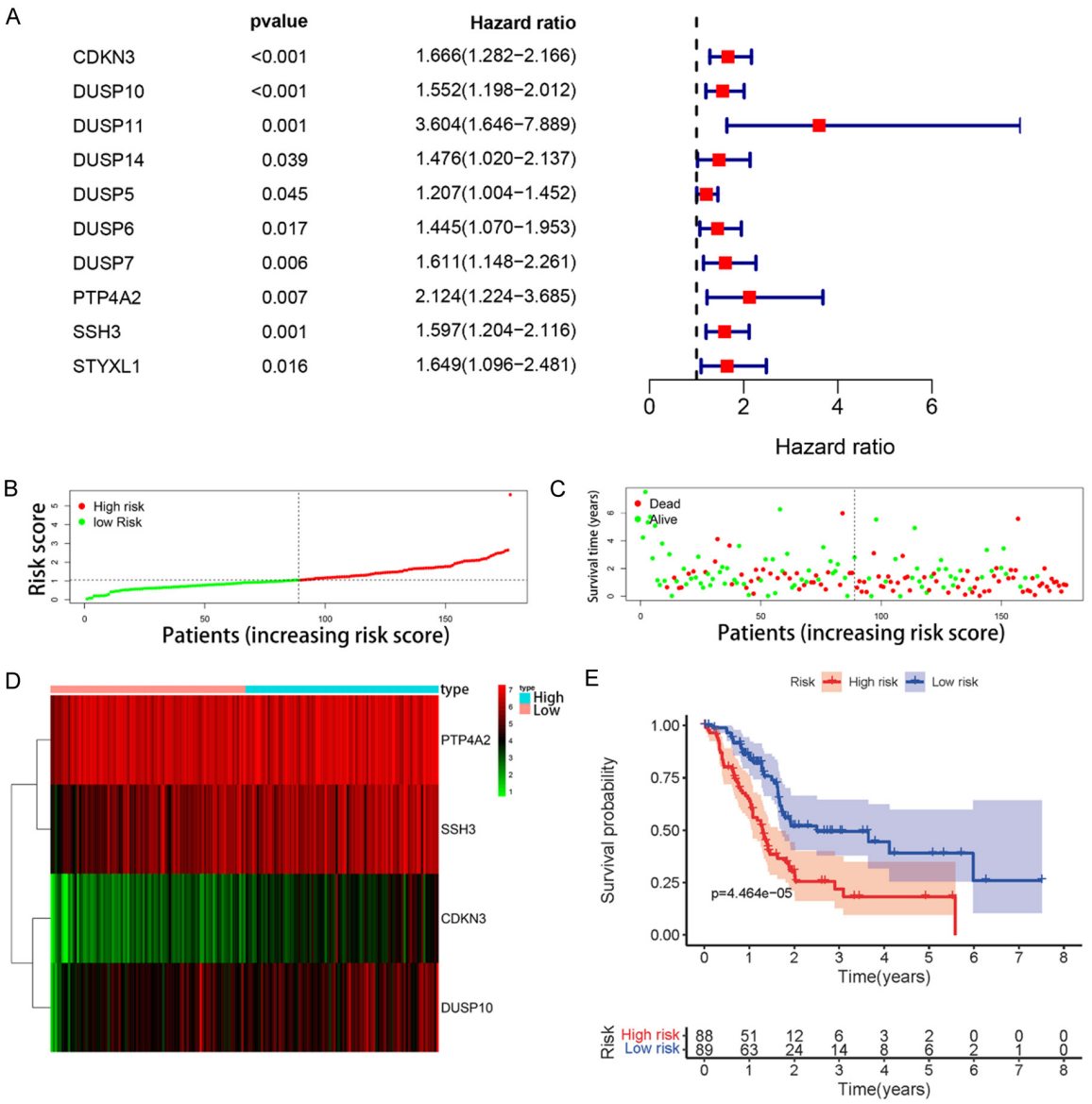

Figure 2. Identifying genes with important prognostic value in PC. (A) Forest plot depicting associations between selected genes and risk value determined via univariate Cox regression analysis. (B) The sample's risk score distribution and (C) the scatterplot based on survival for each sample. Red and green dots, respectively, symbolize life and death. (D) The expression of four genes between the high- and low-risk groups are displayed on the heatmap. (E) Kaplan-Meier survival curve based on the risk model constructed from 4 genes in the TCGA-PAAD cohort.

tive compounds, including AZD1208, BMS-754807, doramapimod, JQ1, LJI308, NU7441, PCI-34051, RO-3306, and tozasertib, exhibited higher efficacy in the high-risk group (**Figure 5A-I**). These findings could have significant implications for personalized treatment strategies in pancreatic cancer.

Expression and survival analysis of SSH3 in PC

Differential expression analysis via the TNMplot platform revealed higher expression levels of DUSP10, PTP4A2, SSH3, and CDKN3 in pancreatic cancer (PC) tissues compared to adjacent normals (**Figures 6A**, S2A-C). Data from the GEPIA database indicated that increased expression of these genes was associated with poorer overall survival (OS) and disease-free survival (DFS) in PC patients (**Figures 6B**, **6C**, S2D-I). Given the known associations of DUSP10, PTP4A2, and CDKN3 with pancreatic cancer (PC), their inclusion strengthens the foundation of our model. However, the role of SSH3 in PC remains less understood.

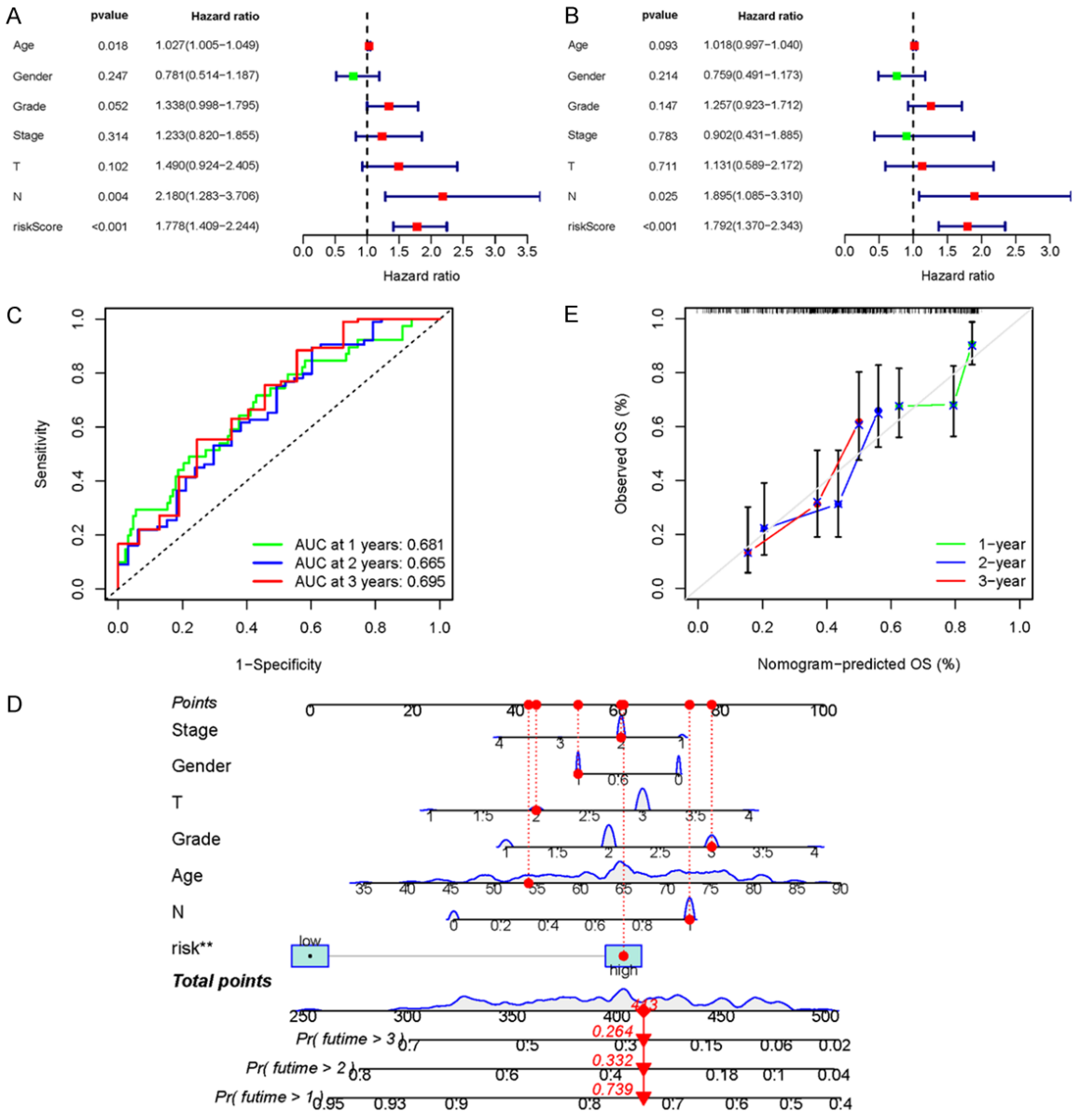

Figure 3. Independent prognostic analysis and construction of nomogram. A. Univariate Cox regression analysis of risk model score and clinical features. B. Multivariate Cox regression analyses of the risk model score and clinical features. C. ROC curve used to evaluate the predictive performance of 1-, 2- and 3-year for overall survival in the TCGA-PAAD cohort. D. Nomogram model constructed by multivariate Cox regression. E. Calibration curve of multivariate Cox regression for the 1-, 2-, and 3-year survival in PC patients.

Consequently, our subsequent research efforts were directed towards elucidating the involvement of SSH3 in the pathogenesis of pancreatic cancer (**Figure 6D-F**). Immunohistochemistry (IHC) data from the Human Protein Atlas (HPA) confirmed SSH3's protein-level elevation in PC tissues (**Figure 6G**). Complementary quantitative PCR (qPCR) and Western blot analyses across five PC cell lines versus human pancreatic ductal epithelial (HPDE) cells underscored SSH3's upregulation, suggesting its role in PC progression (**Figures 6H**, **6I**, S3A).

SSH3 promotes the proliferation and migration of PC cells in vitro

To investigate the impact of SSH3 on PC cell behavior, we employed two specific siRNAs to reduce SSH3 levels in PANC-1 and SW1990 cells, as confirmed by Western blot and qPCR

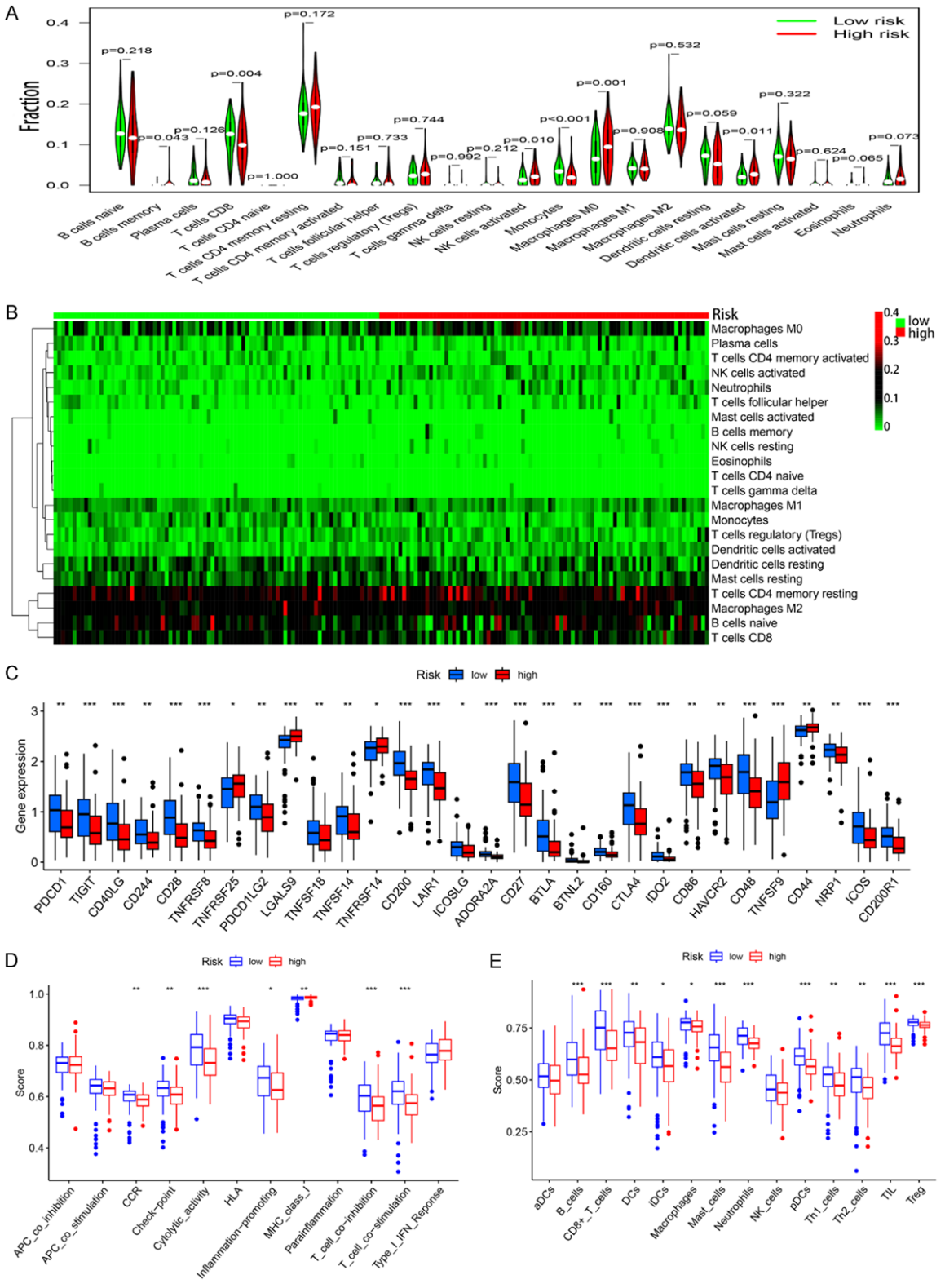

Figure 4. The difference in tumor immunological microenvironment in low- and high-risk groups. A. Comparison of 22 distinct types of immune cells between high- (red) and low-risk group (green). B. Distribution of 22 immune cell types in PC tumor tissues as shown by a bar diagram. C-E. Offered the difference box charts of immune examination sites, immune cell infiltration, and immune function in high-risk and low-risk groups, respectively. *P < 0.05; **P < 0.01; ***P < 0.001.

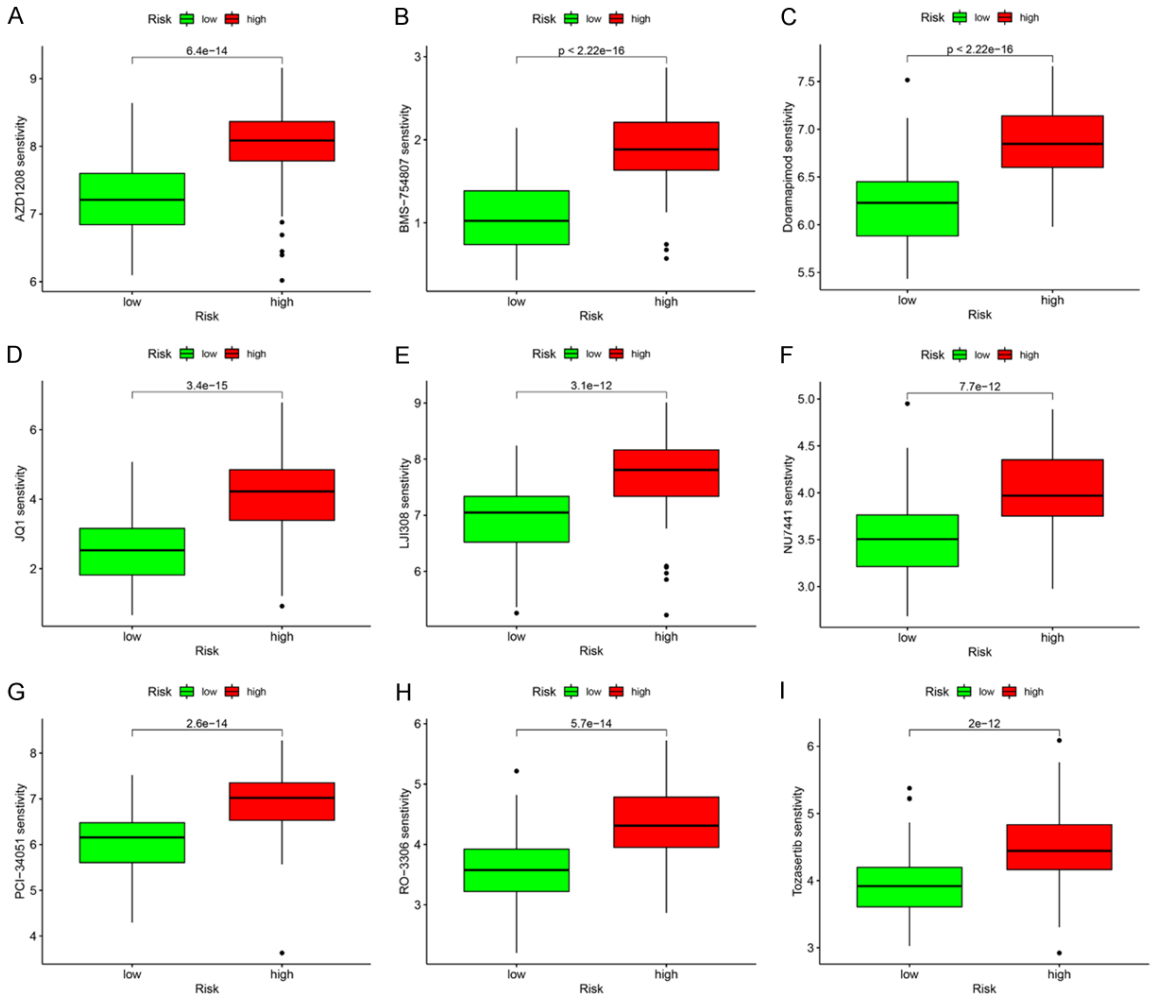

Figure 5. The figures illustrate the relationship between risk groups and drug sensitivity. A. AZD1208; B. BMS-754807; C. Doramapimod; D. JQ1; E. LJI308; F. NU7441; G. PCI-34051; H. RO-3306; I. Tozasertib.

analyses (**Figures 7A**, **7B**, S3B). Following SSH3 knockdown, a notable decrease in cell proliferation was detected using the CCK-8 assay at 96 hours (**Figure 7C**, **7D**). EdU assays corroborated these findings, displaying a significant reduction in EdU-positive cells post-SSH3 suppression (**Figure 7E**, **7F**). Moreover, transwell and wound healing assays demonstrated that SSH3 silencing markedly hindered PC cell migration and invasion (**Figures 7G-I**, S4A, S4B). Western blot analysis post-silencing revealed a decrease in mesenchymal markers vimentin, snail1, and N-cadherin, coupled with an increase in epithelial marker E-cadherin (**Figures 7J**, S3C, S3D). These results collectively suggest a pivotal role for SSH3 in the proliferation, migration, and invasion of PC cells.

SSH3 works by stimulating the NOTCH signaling pathway

GSEA data implicates a potential association of SSH3 with the NOTCH1 signaling pathway in pancreatic cancer (PC) (**Figure 8A**). To explore this, Western blotting was performed, focusing on NICD1 and HES1 - key proteins within the NOTCH1 pathway. Upon silencing SSH3, a noticeable reduction in the levels of these proteins was observed, confirming the initial GSEA data (**Figures 8B**, S3E, S3F). This reduction in NICD1 and HES1 protein levels upon SSH3 silencing directly supports the hypothesis that SSH3 is an activator within the NOTCH1 signaling pathway. To investigate the potential regulatory role of SSH3 in the malignancy of pancreatic cancer via the NOTCH signaling pathway,

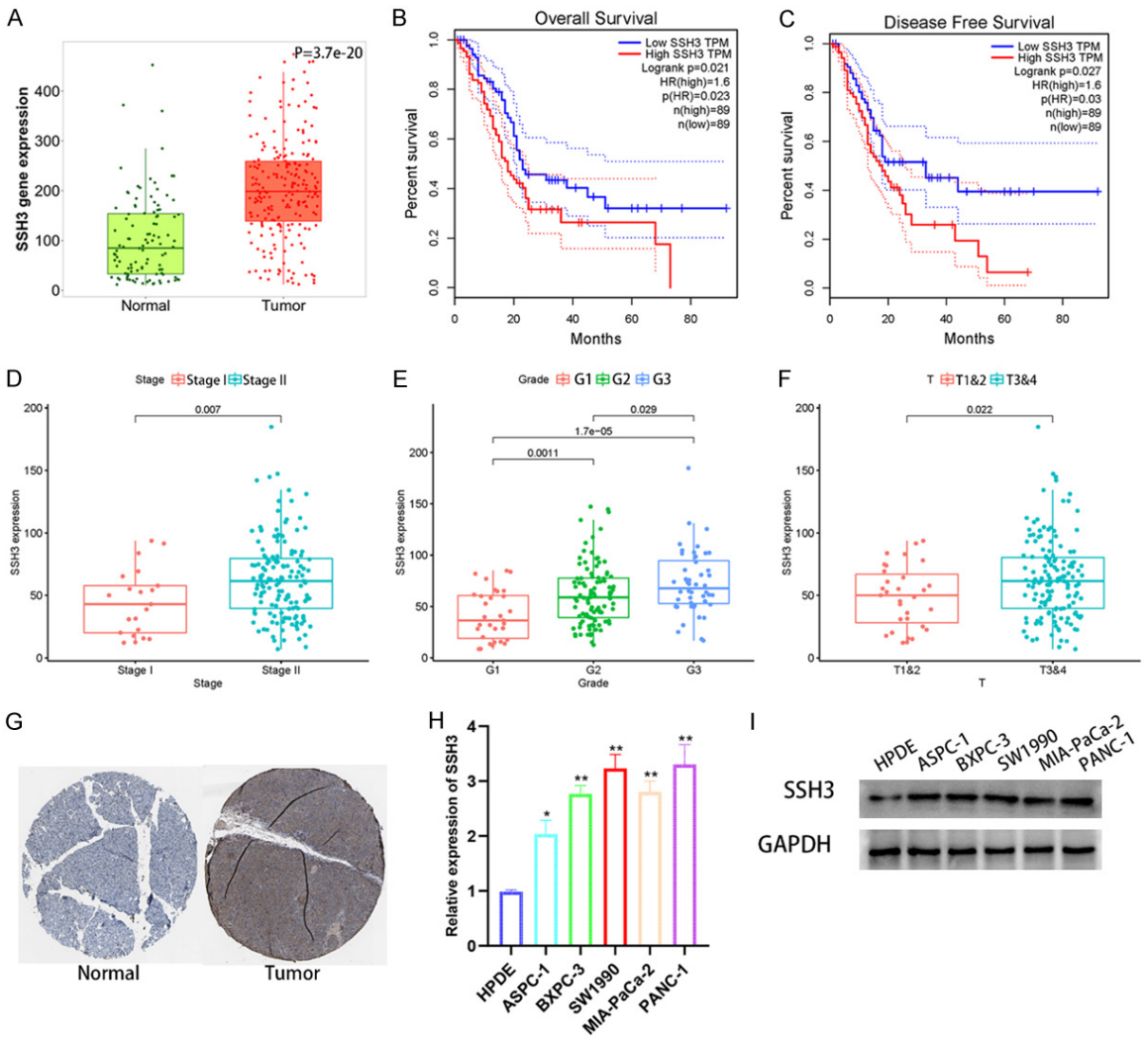

Figure 6. The Expression, OS, and DFS of SSH3 in PC patients. A. The expression of SSH3 in PC and adjacent tissues in TNMplot database. B, C. Kaplan-Meier analysis of the association between SSH3 expression and overall survival and disease-specific survival in the TCGA cohort. D-F. Relationship between the expression of SSH3 and clinical characteristics in PC patients, including stage, grade and T stage. G. Immunohistochemical analysis of SSH3 in pancreatic cancer by the HPA database. H, I. Analysis of SSH3 expression in different cell lines of PDAC and HPDE using qRT-PCR and Western blots (*P < 0.05; **P < 0.01; ***P < 0.001).

we conducted replicative experiments using Jagged-1, an agonist known to activate the NOTCH pathway [15]. CCK-8 and EdU assays demonstrated that Jagged-1 significantly reversed the diminished proliferation caused by SSH3 knockdown in PC cells (**Figure 8C-F**). Additionally, transwell assays showed that Jagged-1 could restore migration and invasion capacities in PC cells, which were impaired due to SSH3 knockdown (**Figures 8G-I**, S4C, S4D). This restorative effect of Jagged-1 on the Notch signaling pathway, particularly after SSH3 silencing, was also observed, hinting at a regulatory loop between the Notch pathway and SSH3 expression (**Figures 8J**, S3G, S3H). Collectively, these findings strongly suggest that SSH3 facilitates PC progression through the NOTCH1 signaling pathway.

SSH3 depletion suppressed tumor growth in vivo

Western blot analysis confirmed the effective knockdown of SSH3 (**Figures 9A**, S3I). In xenograft models, tumors with silenced SSH3 were notably smaller and lighter compared to the control group (**Figure 9B-D**). Histological and immunohistochemistry (IHC) analyses, includ-

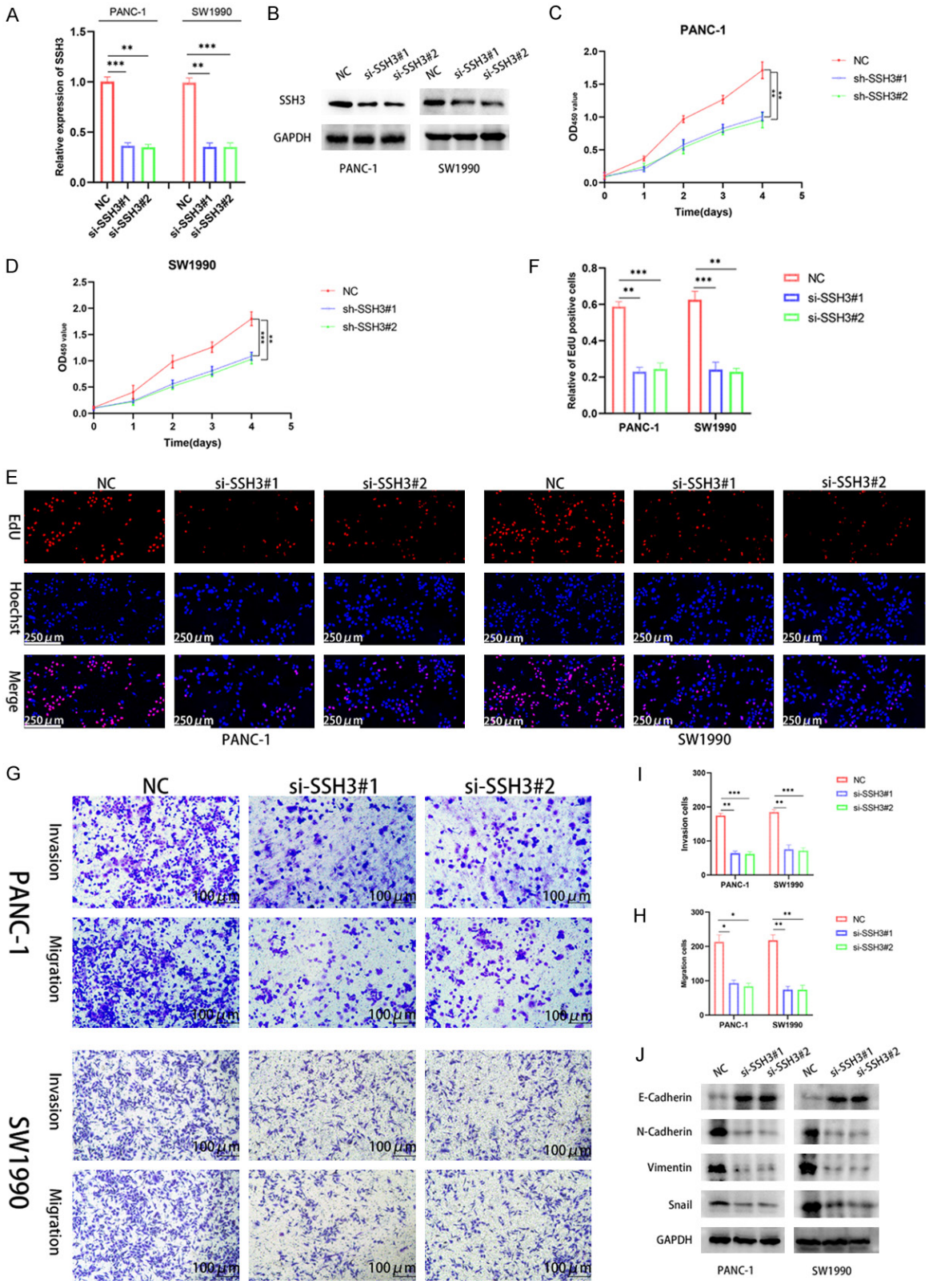

Figure 7. SSH3 knockdown suppresses the proliferation, migration and invasion of PANC-1 and SW1990 cells. A, B. WB and RT-PCR analysis validated the knockdown of SSH3 in PANC-1 and SW1990 cells transfected with NC or si-SSH3. C, D. Cell viability of SSH3 knockdown PANC-1 and SW1990 cells was analysed using the CCK-8 assay. E, F. EdU assay analysis showing the cell proliferation in SSH3 knockdown PANC-1 and SW1990 cells. Scale bar: 250 μm. G-I. Cell migration and invasion were assessed with transwell assay analysis in PANC-1 and SW1990 cells transfected with NC or si-SSH3. Scale bar: 100 μm. J. Expression of EMT-related proteins assessed by western blotting in the PANC-1 and SW1990 cells transfected with NC or si-SSH3, respectively. *P < 0.05; **P < 0.01; ***P < 0.001.

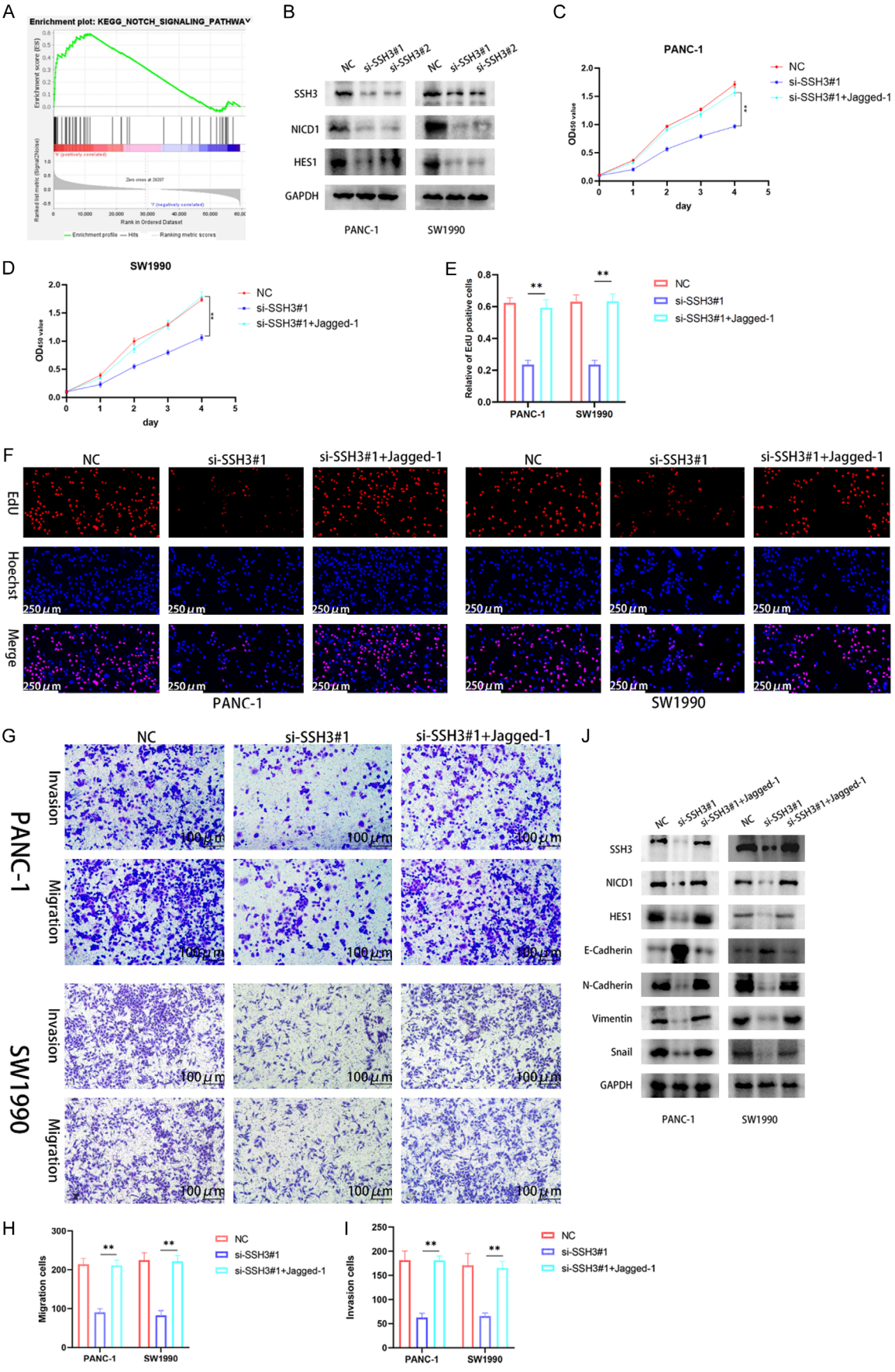
A
Enrichment plot: KEGG_NOTCH_SIGNALING_PATHWAY
B
NC
si-SSH3#1
si-SSH3#2
SSH3
NICD1
HES1
GAPDH
PANC-1
SW1990
C
PANC-1
NC
si-SSH3#1
si-SSH3#1+Jagged-1
OD450 value
day
D
SW1990
E
Relative of EdU positive cells
F
EdU
Hoechst
Merge
250 μm
G
Invasion
Migration
100 μm
J
E-Cadherin
N-Cadherin
Vimentin
Snail
H
Migration cells
I
Invasion cells

Figure 8. SSH3 promotes the proliferation, migration, and invasion of PANC-1 and SW1990 cells via activating the NOTCH pathway in vitro. A. The GSEA results showed a connection between SSH3 expression and the NOTCH signaling pathway. B. The protein levels of NICD1 and its target genes. Representative Western blots for SSH3 and NOTCH pathway markers (NOTCH1 and HES1) in PANC-1 and SW1990 cells transfected with NC or si-SSH3. C, D. CCK-8 assay analysis illustrate the effects of the NOTCH pathway agonist Jagged-1 on SSH3-mediated migration of PANC-1 and SW1990 cells. E, F. EdU assays illustrate the effects of the NOTCH pathway agonist Jagged-1 on SSH3-mediated migration of PANC-1 and SW1990 cells. Scale bar: 250 μm. G-I. Transwell assays illustrate the effects of the NOTCH pathway agonist Jagged-1 on SSH3-mediated migration of PANC-1 and SW1990 cells. Scale bar: 100 μm. J. Expression of SSH3, NOTCH1 and HES1 and EMT-related proteins assessed by western blotting in the PANC-1 and SW1990 cells. *P < 0.05; **P < 0.01; ***P < 0.001.

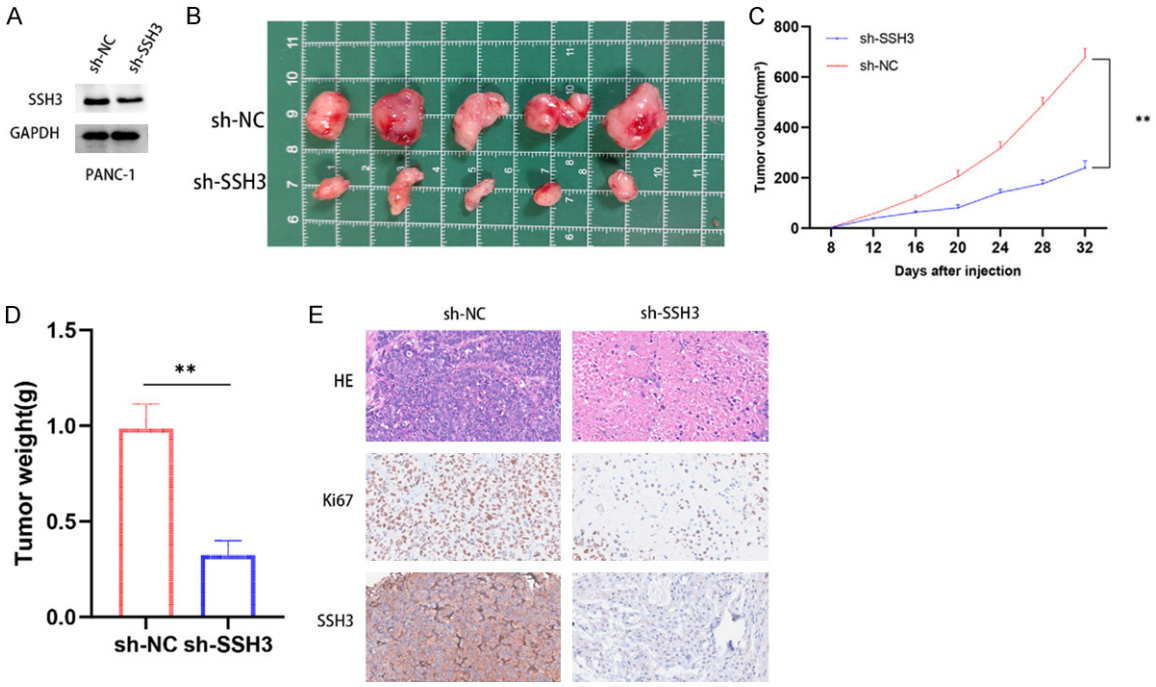

Figure 9. In vivo mice studies showed that SSH3 depletion suppressed tumor growth. A. The expression of SSH3 in PANC-1 cells transfection with SSH3 shRNA. B. Tumor size is shown in sh-SSH3 groups and the control groups. C, D. Both the weight and volume of subcutaneous tumors that were xenografted onto nude mice at the specified times after injection. E. HE and IHC results of the indicated proteins in xenografted PC tumors. Scale bar = 50 μm. *P < 0.05; **P < 0.01; ***P < 0.001.

ing HE staining and SSH3 and Ki67 antibodies, showed decreased expression in the sh-SSH3 group (**Figure 9E**). These results collectively demonstrate that SSH3 promotes pancreatic cancer (PC) cell proliferation and migration through activation of the Notch signaling pathway, thereby playing a crucial role in tumor progression.

Discussion

Pancreatic cancer (PC), often diagnosed at an advanced stage, is anticipated to become the second most common cause of cancer-related death [16]. Currently, the mainstays of PC treatment are chemotherapy and surgery, yet only about 15%-20% of patients are eligible for surgical intervention at diagnosis [17]. Regrettably, post-surgical recurrence is high, with approximately 75% of patients experiencing relapse within two years, suggesting prevalent micrometastatic disease even in those who undergo resection [18]. The origin of most PDAC (pancreatic ductal adenocarcinoma) cases can be traced to pancreatic intraepithelial neoplasia (PanIN), which progresses to PDAC through a sequence of genetic changes [19, 20]. Considering the typically late-stage diagnosis of PC, there is a pressing need to enhance early detection methods, reflecting an ongoing effort to improve patient outcomes in the context of advanced or metastatic disease [21].

Mitogen-Activated Protein Kinases (MAPKs) are pivotal in cell functioning, modulating a broad array of molecular effectors [22]. Dual-specificity phosphatases (DUSPs) play a crucial role as key regulators, dephosphorylating essential signaling molecules like MAPKs. This action influences diverse biological processes, ranging from signaling pathways to protein stability, and is implicated in numerous diseases, including cancer [23, 24]. Increasing evidence points to the dysregulation of DUSPs as a common characteristic in cancer, significantly impacting both its initiation and progression [23, 24]. Despite extensive research, many DUSPs remain underexplored in oncology, underscoring the necessity for continued studies to fully understand their roles in cancer development and progression.

In this study, differential analysis of dual-specificity phosphatases (DUSPs) across 171 normal tissues and 178 pancreatic cancer (PC) tumors identified 20 differentially expressed genes (DEGs). Univariate and multivariate Cox regression analyses highlighted four genes - DUSP10, PTP4A2, SSH3, and CDKN3 - as significantly correlated with overall survival (OS) in PC. The efficacy of the prognostic model was further validated using receiver operating characteristic (ROC) curve analysis. Functional analyses shed light on the biological implications of these genes within the prognostic models, providing insights for tumor immune analysis and the prediction of potential chemical drugs, thereby paving the way for personalized therapeutic approaches. Specifically, DUSP10 was observed to modulate cell proliferation via JNK signaling and ERK1/2 pathways [25, 26]. PTP4A2 influenced AKT phosphorylation, affecting cellular proliferation processes, while CDKN3's interaction with PSMD12 and GID2 was linked to cancer progression [27-29]. SSH3, encoded on chromosome 11q13.2, is a member of the SSH phosphatase family, known for dephosphorylating and activating ADF/cofilin [30, 31]. While SSH1's upregulation in various tumors has been established, the role of SSH3 in PC remained elusive [32-34]. Studies have shown SSH3's involvement in cancer progression via the LIMK1/Rac signaling pathways in colorectal cancer and the activation of the FGF1/FGFR pathway in hepatocellular carcinoma [30, 35]. Given these gaps, our research focused on SSH3's function in PC. Elevated expression of SSH3 in PC, relative to human pancreatic ductal epithelial (HPDE) cells, was confirmed by qPCR and Western blotting. SSH3 knockdown in PC cells led to marked reductions in proliferation and invasion, and the subcutaneous injection of SSH3-knockout PANC-1 cells into nude mice significantly suppressed tumor growth. These findings underscore the potential of SSH3 as a therapeutic target in PC. Through in-depth analysis, this study contributes to the broader understanding of PC's molecular dynamics, with a particular emphasis on SSH3's role in disease progression and response to treatment. Our findings highlight the importance of SSH3 in PC pathogenesis and open new avenues for targeted therapies in pancreatic cancer.

The Notch signaling pathway, a crucial player in embryogenesis, exhibits paradoxical roles in oncogenesis as both a tumor suppressor and an oncogene [36]. This pathway is activated upon binding of the Notch receptor to its ligand, triggering proteolytic cleavages that release the Notch intracellular domain (NICD) [37]. This activation promotes cancer progression through downstream target gene stimulation [38]. Our GSEA results indicated that SSH3 expression is significantly enriched in the NOTCH signaling pathway. Further investigation using Western blot analysis demonstrated that SSH3 modulates NICD1 and HES1 levels, two key elements within this pathway. Additionally, the application of the Notch agonist Jagged-1 was found to counteract the effects of SSH3 knockdown on cancer cell malignancy.

This study, utilizing The Cancer Genome Atlas (TCGA) dataset to develop a prognostic model for pancreatic cancer (PC), acknowledges certain limitations. The sample size, comprising 178 PC samples, points to the need for larger cohorts to strengthen the analytical robustness. Moreover, while SSH3's expression was analyzed through Western blotting and qPCR, more in-depth research is essential to fully understand the interaction between SSH3 and the Notch signaling pathway in PC progression. Consequently, these findings should be viewed as preliminary, emphasizing the need for more comprehensive studies to validate the implicated pathways in PC.

Acknowledgements

This work was supported by National Natural Science Foundation of China (No. 82372948), and the Dongguan Science and Technology of Social Development Key Program (No. 20231800932412).

Disclosure of conflict of interest

None.

Address correspondence to: Jianxin Jiang, Department of Hepatobiliary, Pancreatic and Splenic Surgery, The Tenth Affiliated Hospital, Southern Medical University (Dongguan People's Hospital), No. 78, Wan Road, Xinguyong, Wanjiang Street, Dongguan 523018, Guangdong, China. Tel: +86-0769-28636957; Fax: +86-0769-28636957; E-mail: rm002979@whu.edu.cn

References

[1] Klein AP. Pancreatic cancer epidemiology: understanding the role of lifestyle and inherited risk factors. Nat Rev Gastroenterol Hepatol 2021; 18: 493-502.

[2] Guccini I, Tang G, To TT, Di Rito L, Le Blanc S, Strobel O, D'Ambrosio M, Pasquini E, Bolis M, Silva P, Kabakci HA, Godbersen S, Alimonti A, Schwank G and Stoffel M. Genetic ablation of ketohexokinase C isoform impairs pancreatic cancer development. iScience 2023; 26: 107368.

[3] Zhou B, Xu JW, Cheng YG, Gao JY, Hu SY, Wang L and Zhan HX. Early detection of pancreatic cancer: where are we now and where are we going? Int J Cancer 2017; 141: 231-241.

[4] Caputo D, Quagliarini E, Coppola A, La Vaccara V, Marmiroli B, Sartori B, Caracciolo G and Pozzi D. Inflammatory biomarkers and nanotechnology: new insights in pancreatic cancer early detection. Int J Surg 2023; 109: 2934-2940.

[5] Nakamura K, Zhu Z, Roy S, Jun E, Han H, Munoz RM, Nishiwada S, Sharma G, Cridebring D, Zenhausern F, Kim S, Roe DJ, Darabi S, Han IW, Evans DB, Yamada S, Demeure MJ, Becerra C, Celinski SA, Borazanci E, Tsai S, Kodera Y, Park JO, Bolton JS, Wang X, Kim SC, Von Hoff D and Goel A. An exosome-based transcriptomic signature for noninvasive, early detection of patients with pancreatic ductal adenocarcinoma: a multicenter cohort study. Gastroenterology 2022; 163: 1252-1266, e1252.

[6] Lucas AL and Kastrinos F. Screening for pancreatic cancer. JAMA 2019; 322: 407-408.

[7] Park W, Chawla A and O'Reilly EM. Pancreatic cancer: a review. JAMA 2021; 326: 851-862.

[8] Luo J. KRAS mutation in pancreatic cancer. Semin Oncol 2021; 48: 10-18.

[9] Huang CY and Tan TH. DUSPs, to MAP kinases and beyond. Cell Biosci 2012; 2: 24.

[10] Wilczek MP, Armstrong FJ, Geohegan RP, Mayberry CL, DuShane JK, King BL and Maginnis MS. The MAPK/ERK pathway and the role of DUSP1 in JCPyV infection of primary astrocytes. Viruses 2021; 13: 1834.

[11] Ríos P, Nunes-Xavier CE, Tabernero L, Köhn M and Pulido R. Dual-specificity phosphatases as molecular targets for inhibition in human disease. Antioxid Redox Signal 2014; 20: 2251-2273.

[12] Li X, Jin F and Li Y. A novel autophagy-related lncRNA prognostic risk model for breast cancer. J Cell Mol Med 2021; 25: 4-14.

[13] Zhu J, Mou Y, Ye S, Hu H, Wang R, Yang Q and Hu Y. Identification of a six-gene SLC family signature with prognostic value in patients with lung adenocarcinoma. Front Cell Dev Biol 2021; 9: 803198.

[14] Xu S, Liu D, Chang T, Wen X, Ma S, Sun G, Wang L, Chen S, Xu Y and Zhang H. Cuproptosis-associated lncRNA establishes new prognostic profile and predicts immunotherapy response in clear cell renal cell carcinoma. Front Genet 2022; 13: 938259.

[15] Jundt F, Pröbsting KS, Anagnostopoulos I, Muehlinghaus G, Chatterjee M, Mathas S, Bargou RC, Manz R, Stein H and Dörken B. Jagged1-induced Notch signaling drives proliferation of multiple myeloma cells. Blood 2004; 103: 3511-3515.

[16] Collisson EA, Bailey P, Chang DK and Biankin AV. Molecular subtypes of pancreatic cancer. Nat Rev Gastroenterol Hepatol 2019; 16: 207-220.

[17] Pancreatic cancer. Nat Rev Dis Primers 2016; 2: 16023.

[18] Halbrook CJ, Lyssiotis CA, Pasca di Magliano M and Maitra A. Pancreatic cancer: advances and challenges. Cell 2023; 186: 1729-1754.

[19] Hruban RH and Fukushima N. Pancreatic adenocarcinoma: update on the surgical pathology of carcinomas of ductal origin and PanINs. Mod Pathol 2007; 20 Suppl 1: S61-70.

[20] Mello SS, Flowers BM, Mazur PK, Lee JJ, Müller F, Denny SK, Ferreira S, Hanson K, Kim SK, Greenleaf WJ, Wood LD and Attardi LD. Multifaceted role for p53 in pancreatic cancer suppression. Proc Natl Acad Sci U S A 2023; 120: e2211937120.

[21] Mizrahi JD, Surana R, Valle JW and Shroff RT. Pancreatic cancer. Lancet 2020; 395: 2008-2020.

[22] Khoubai FZ and Grosset CF. DUSP9, a dual-specificity phosphatase with a key role in cell biology and human diseases. Int J Mol Sci 2021; 22: 11538.
[23] Chen HF, Chuang HC and Tan TH. Regulation of dual-specificity phosphatase (DUSP) ubiquitination and protein stability. Int J Mol Sci 2019; 20: 2668.
[24] Gao PP, Qi XW, Sun N, Sun YY, Zhang Y, Tan XN, Ding J, Han F and Zhang Y. The emerging roles of dual-specificity phosphatases and their specific characteristics in human cancer. Biochim Biophys Acta Rev Cancer 2021; 1876: 188562.
[25] Liu M, Qin Y, Hu Q, Liu W, Ji S, Xu W, Fan G, Ye Z, Zhang Z, Xu X, Yu X and Zhuo Q. SETD8 potentiates constitutive ERK1/2 activation via epigenetically silencing DUSP10 expression in pancreatic cancer. Cancer Lett 2021; 499: 265-278.
[26] He G, Zhang L, Li Q and Yang L. miR-92a/DUSP10/JNK signalling axis promotes human pancreatic cancer cells proliferation. Biomed Pharmacother 2014; 68: 25-30.
[27] Hardy S, Wong NN, Muller WJ, Park M and Tremblay ML. Overexpression of the protein tyrosine phosphatase PRL-2 correlates with breast tumor formation and progression. Cancer Res 2010; 70: 8959-8967.
[28] Stephens B, Han H, Hostetter G, Demeure MJ and Von Hoff DD. Small interfering RNA-mediated knockdown of PRL phosphatases results in altered Akt phosphorylation and reduced clonogenicity of pancreatic cancer cells. Mol Cancer Ther 2008; 7: 202-210.
[29] Deng X, Ma J, Zhou W, Yuan Y, Wang B and Meng X. GID2 interacts with CDKN3 and regulates pancreatic cancer growth and apoptosis. Lab Invest 2023; 103: 100122.
[30] Hu YH, Lu YX, Zhang ZY, Zhang JM, Zhang WJ, Zheng L, Lin WH, Zhang W and Li XN. SSH3 facilitates colorectal cancer cell invasion and metastasis by affecting signaling cascades involving LIMK1/Rac1. Am J Cancer Res 2019; 9: 1061-1073.
[31] Niwa R, Nagata-Ohashi K, Takeichi M, Mizuno K and Uemura T. Control of actin reorganization by Slingshot, a family of phosphatases that dephosphorylate ADF/cofilin. Cell 2002; 108: 233-246.
[32] Sousa-Squiavinato ACM, Vasconcelos RI, Gehren AS, Fernandes PV, de Oliveira IM, Boroni M and Morgado-Díaz JA. Cofilin-1, LIMK1 and SSH1 are differentially expressed in locally advanced colorectal cancer and according to consensus molecular subtypes. Cancer Cell Int 2021; 21: 69.
[33] Daryabari SS, Safaralizadeh R, Hosseinpourfeizi M, Moaddab Y and Shokouhi B. Overexpression of SSH1 in gastric adenocarcinoma and its correlation with clinicopathological features. J Gastrointest Oncol 2018; 9: 728-733.
[34] Maimaiti Y, Maimaitiming M, Li Y, Aibibula S, Ainiwaer A, Aili A, Sun Z and Abudureyimu K. SSH1 expression is associated with gastric cancer progression and predicts a poor prognosis. BMC Gastroenterol 2018; 18: 12.
[35] Shi QS, Zhang YH, Long J, Qian ZL and Hu CX. SSH3 promotes malignant progression of HCC by activating FGF1-mediated FGF/FGFR pathway. Eur Rev Med Pharmacol Sci 2020; 24: 11561-11568.
[36] Misiorek JO, Przybyszewska-Podstawka A, Kałafut J, Paziewska B, Rolle K, Rivero-Müller A and Nees M. Context matters: NOTCH signatures and pathway in cancer progression and metastasis. Cells 2021; 10: 94.
[37] Luo Z, Mu L, Zheng Y, Shen W, Li J, Xu L, Zhong B, Liu Y and Zhou Y. NUMB enhances Notch signaling by repressing ubiquitination of NOTCH1 intracellular domain. J Mol Cell Biol 2020; 12: 345-358.
[38] Chen S, Cai K, Zheng D, Liu Y, Li L, He Z, Sun C and Yu C. RHBDL2 promotes the proliferation, migration, and invasion of pancreatic cancer by stabilizing the N1ICD via the OTUD7B and activating the Notch signaling pathway. Cell Death Dis 2022; 13: 945.

Table S1A. SiRNAs used in this research

Name	Sequences
si-SSH3#1	5'-CCTGCTGGTAGTTTCTACACGAGAA-3'
si-SSH3#2	5'-AGTGACATGCCAGAGGTCTTCTCTT-3'

Table S1B. ShRNA used in this research

Name	Sequences
Sh-SSH3	CCTGCTGGTAGTTTCTACA

Table S1C. Primers used in this research

Name	Direction	Sequences (5'-3')
SSH3	Forward	CCTGCTGGTAGTTTCTACACG
	Reverse	CACCTGGGTGTCACTCCAGA
GAPDH	Forward	TGTGGGCATCAATGGATTTGG
	Reverse	ACACCATGTATTCCGGGTCAAT

Table S1D. Antibodies used in this research

Name	Host	Catalogue
SSH3	Rabbit	sc-374560, San Juan Ranch, Dallas, USA
Snail1	Rabbit	A5243, ABclonal, Wuhan, China
Vimentin	Rabbit	10366-1-AP, Proteintech, Wuhan, China
NOTCH1	Rabbit	20687-1-AP, Proteintech, Wuhan, China
HES1	Rabbit	A11718, ABclonal, Wuhan, China
N-Cadherin	Rabbit	22018-1-AP, Proteintech, Wuhan, China
E-Cadherin	Rabbit	20874-1-AP, Proteintech, Wuhan, China
GAPDH	Rabbit	10494-1-AP, Proteintech, Wuhan, China
Anti-Rabbit IgG	/	AS014, ABclonal, Wuhan, China
Anti-Mouse IgG	/	AS003, ABclonal, Wuhan, China

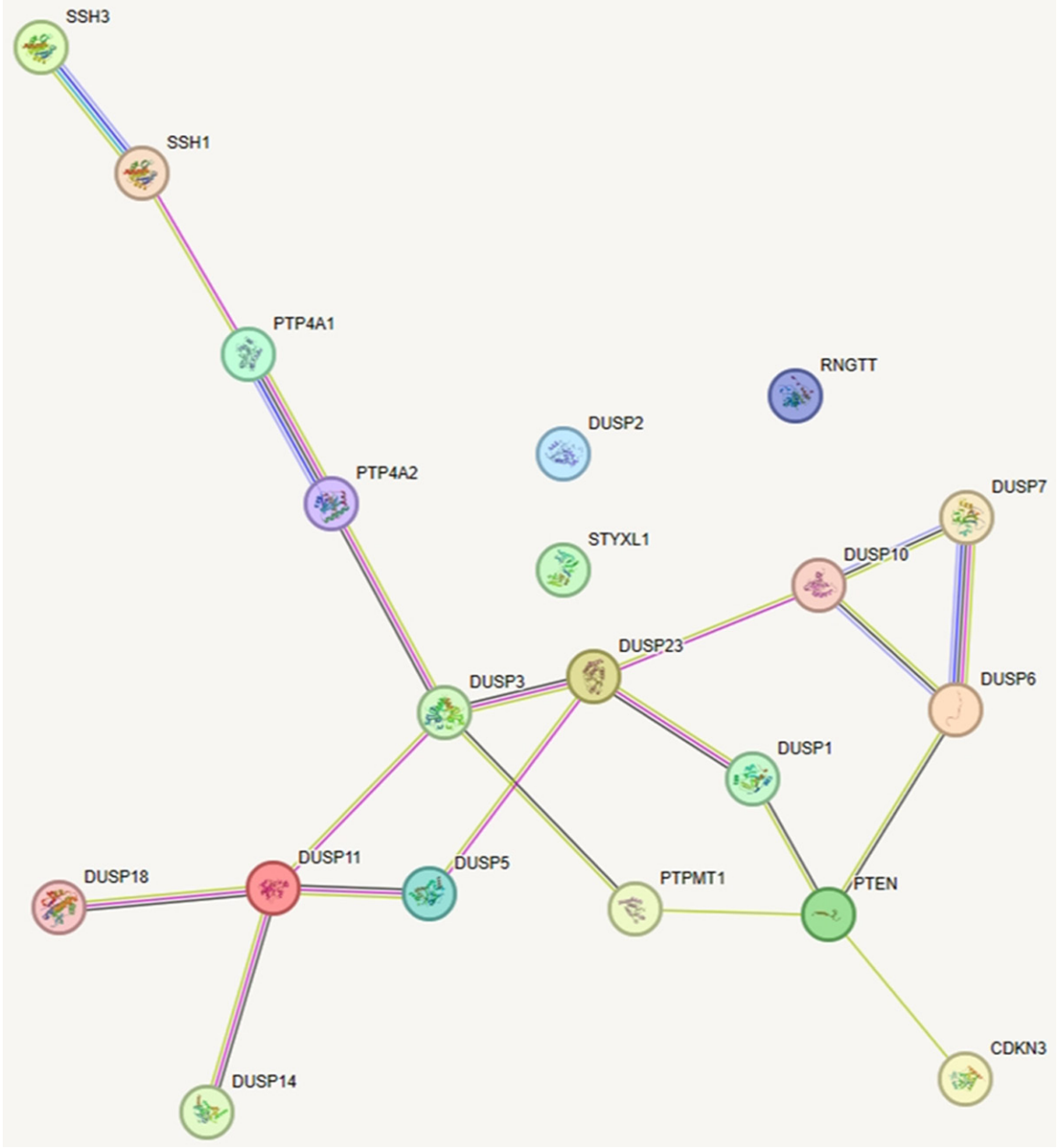

Figure S1. Construction of PPI network to identify 20 DEGs.

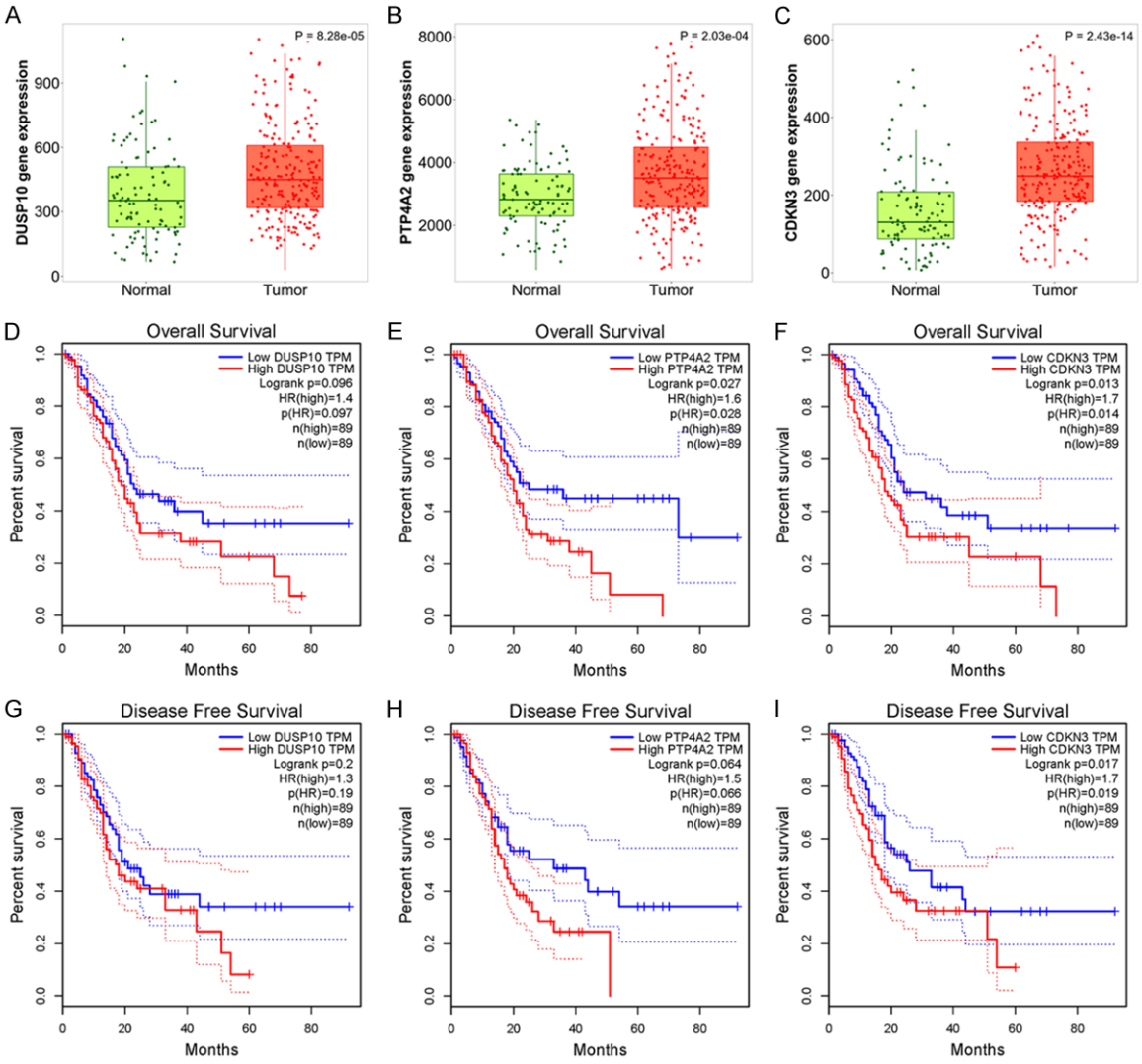

Figure S2. Expression, OS and DFS of the SSH3 in PC patients. A. The expression of DUSP10 in PC tissues and adjacent non-tumor tissues. B. The expression of PTP4A2 in PC tissues and adjacent non-tumor tissues. C. The expression of CDKN3 in PC tissues and adjacent non-tumor tissues. D. Kaplan-Meier survival analysis of DUSP10 in the TCGA cohort. E. Kaplan-Meier survival analysis of PTP4A2 in the TCGA cohort. F. Kaplan-Meier survival analysis of CDKN3 in the TCGA cohort. G. DFS of the DUSP10 in PC patients. H. DFS of the PTP4A2 in PC patients. I. DFS of the CDKN3 in PC patients.

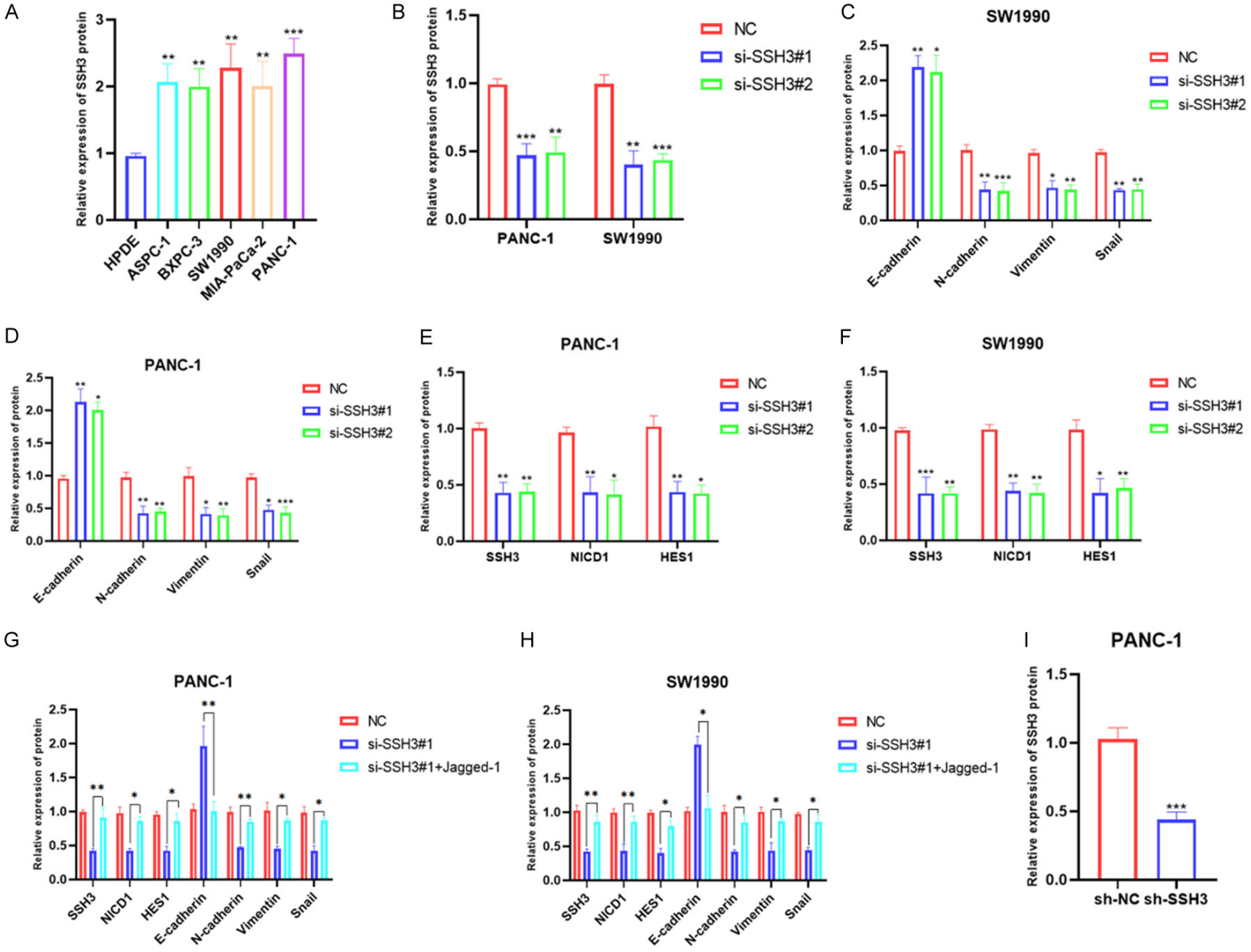

Figure S3. Quantified all Western blots. A. Quantified SSH3 expression in PC cells and HPDE using Western blots. B. Quantified SSH3 expression in PANC-1 and SW1990 cells transfected with NC or si-SSH3 by Western blot. C, D. Quantified expression of EMT-related proteins in PANC-1 and SW1990 cells transfected with NC

or si-SSH3 by Western blotting. E, F. Quantified protein levels of NICD1 and its target genes in PANC-1 and SW1990 cells transfected with NC or si-SSH3. G, H. Quantified expression of Expression of SSH3, NOTCH1 and HES1 and EMT-related proteins in PC cells by Western blotting. I. Quantified expression of SSH3 in PANC-1 cells transfected with sh-NC and sh-SSH3 by Western blots.

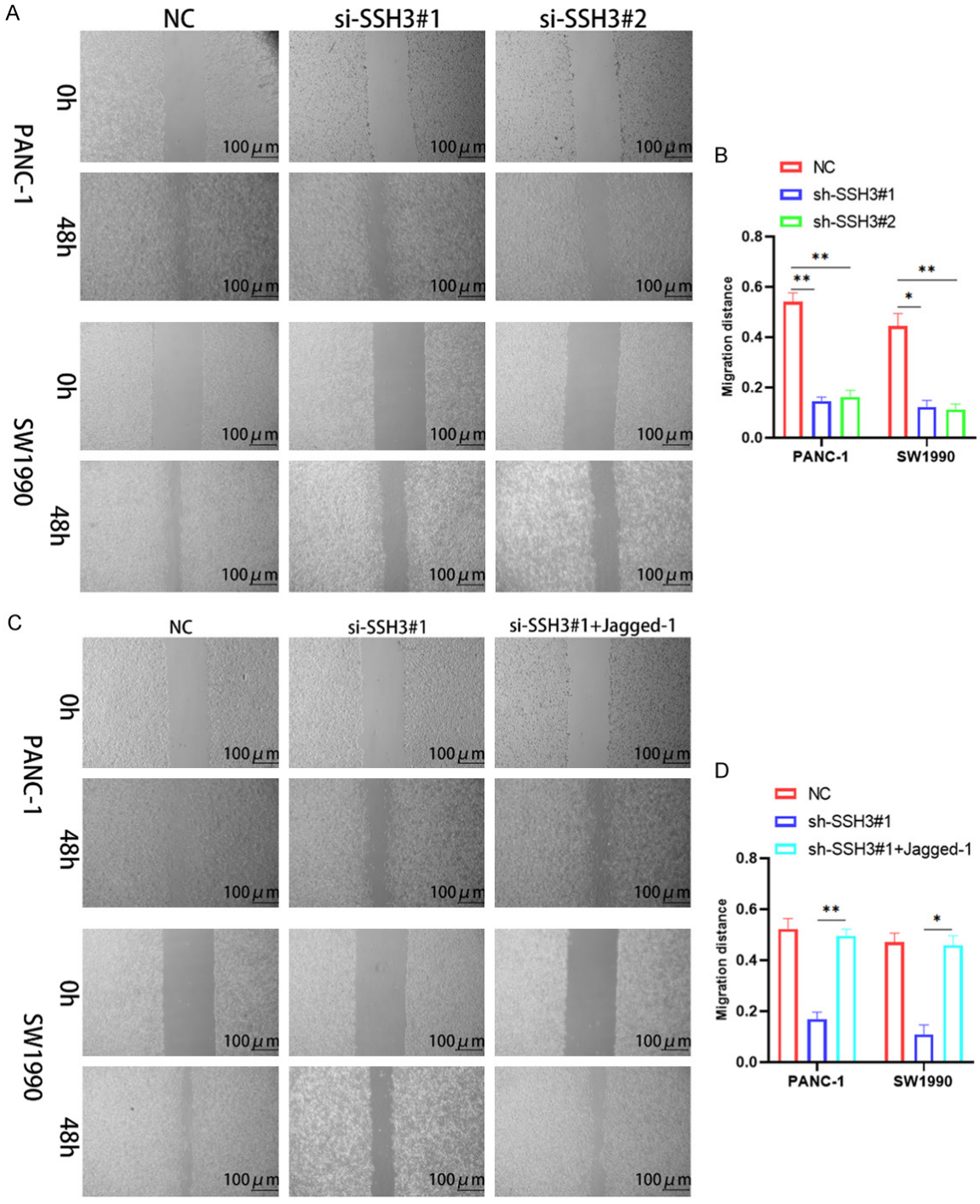

Figure S4. A, B. Wound healing analysis assessed cell migration and invasion in PANC-1 and SW1990 cells transfected with NC or si-SSH3. Scale bar: 100 μm. C, D. Wound healing analysis illustrate the effects of the NOTCH pathway agonist Jagged-1 on SSH3-mediated migration of PANC-1 and SW1990 cells. Scale bar: 100 μm.